Nucleation and growth of InN by high-pressure chemical vapor deposition: Optical monitoring

Vincent Woods, Jayantha Senawirante, and Nikolaus Dietz[a)]
Georgia State University, Department of Physics and Astronomy, Atlanta, Georgia 30303-3083

(Received 31 January 2005; accepted 19 April 2005; published 25 July 2005)

The growth of high quality, stoichiometric InN presents a challenge because of the volatility of atomic nitrogen. To overcome the associated difficulties, a high-pressure chemical vapor deposition (HPCVD) system has been developed, which has opened the avenue for achieving stoichiometric single-phase surface compositions for materials such as InN for which thermal decomposition pressures are large at optimum processing temperatures. We report results obtained during InN growth in the pressure range of 2–15 bar to achieve the earlier objectives and to obtain insights into the InN nucleation and growth process. Using real-time optical ultraviolet absorption spectroscopy, we characterized the chemistry of the gas-phase precursors as functions of flow, pressure, and temperature. Highly surface sensitive probing on InN nucleation and steady state growth is achieved by principal-angle-reflectance spectroscopy, allowing the characterization of surface chemistry at a submonolayer level. The InN layers grown at lower temperatures exhibit an absorption edge at 1.85 eV, which is shifted towards lower energies as the growth temperatures increase. Absorption edges as low as 0.7 eV are observed, values reported for molecular beam epitaxy-grown InN material. The real-time optical monitoring techniques employed demonstrated their superiority in optimizing and controlling the growth process, as well as in gaining insight in gas phase and surface chemistry processes during HPCVD. © *2005 American Vacuum Society.* [DOI: 10.1116/1.1943444]

I. INTRODUCTION

Device structures based on group III-nitride compound alloys have attracted much interest in recent years due to their wide range of applications that can not be accomplished with present Si and group III–P/As materials technology. At present, the growth of III-nitrides is mostly performed using low-pressure deposition techniques such as molecular beam epitaxy (MBE),[1–3] organometallic chemical vapor deposition[4,5] (OMCVD) or variations of both. However, low-pressure deposition processes are limited to regimes where the partial pressures of the constituents do not differ vastly and the decomposition process can be countered by off-equilibrium processing conditions. The application of these techniques for the growth of InN and related indium rich III–N alloys becomes a major challenge due to their stoichiometric instabilities and low dissociation temperatures, leading to inconsistent and process dependent materials properties. Even for the binary InN compound itself, many of the fundamental properties are still debated. The considerable uncertainty over the band gap of InN,[1,6–8] the influence of the intrinsic materials point defect chemistry on the optical and electrical properties,[9] and the effect of extrinsic impurities such oxygen on the band gap,[10,11] show the lack of understanding in this system. Controversial reviews of the present status of InN growth and characterization were provided by Bhuiyan *et al.*[9] and Davydov *et al.*,[12] implying that different approaches for the growth of In-rich group-III-nitride alloys need to be explored in order to improve the structural and optical properties of InN and related alloys.

Recent studies in the indium-nitrogen system[13] show much uncertainties in the *p*-*T*-*x* relations due to missing experimental validation. However, studies of the nitrogen pressure needed to prevent thermal decomposition of bulk InN provided a relationship given by[14]

$$p(\mathrm{N}_2) \rightarrow p_0 \exp\left[-\frac{\Delta H_r}{R}\left(\frac{1}{T}-\frac{1}{T_0}\right)\right]. \qquad (1)$$

The relation indicates that in the pressure range $p_{\mathrm{N}_2} \leqslant 10^2$ bar and for substrate temperatures 900 K the surface decomposition of InN can be effectively suppressed. This approach was implemented at GSU, growing group III-nitrides at elevated pressures focusing on InN, which is the most challenging material system, since the equilibrium vapor pressure of nitrogen over InN is much higher compared to AlN and GaN.[15]

The integration of optical monitoring capabilities for gas flow, gas phase decomposition kinetics, as well as surface

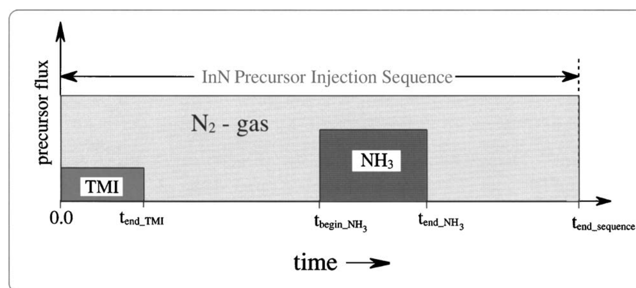

FIG. 1. Schematic representation of a precursor cycle sequence used for the growth of InN via the precursors TMI and ammonia.

[a)]Electronic mail: ndietz@gsu.edu

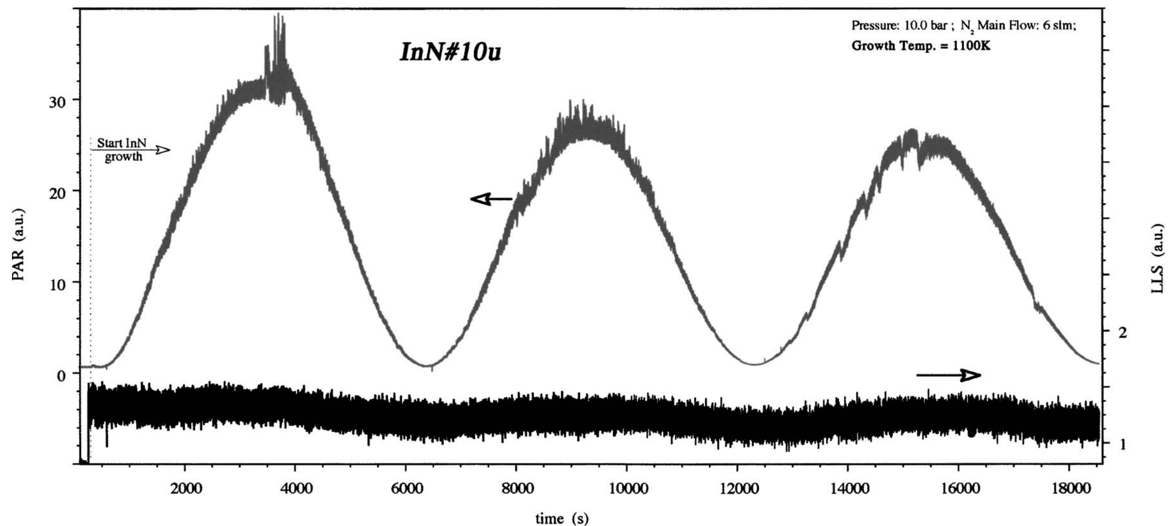

FIG. 2. Real-time optical monitoring of InN growth by PAR and LLS.

reactions is crucial to gain insights in the growth process and in order to control the process on a submonolayer level in real time. In addition, the growth of InN at high pressures requires serious attention towards *minimization* of gas phase reactions, extracting sufficient organometallic (OM) nutrients from the OM bubblers, and embedding the precursor flows in the reactor main stream. Those considerations led to the design of a pulsed precursor injection scheme, which is essential for

- *compression of precursors to reactor pressure*,
- *minimization of gas phase reactions*,
- *engineered nucleation kinetics and layer growth, and*
- *analyzing the gas-phase and surface decomposition dynamics in real-time*.

II. EXPERIMENT

A high-pressure flow channel reactor with incorporated real time optical characterization capabilities[16–21] is utilized to study and optimize the InN nucleation and growth.[22–25] Ammonia (NH_3) and trimethlyindium (TMI) are employed in pulsed injection scheme as schematically depicted in Fig. 1. The precursor pulses are embedded and temporally controlled in a high pressure main stream, consisting of ultrapure nitrogen. The total flow through the reactor as well as the reactor pressure are kept constant at all time.

Integrated optical access ports along the center axis of the substrates are used to monitor the flow kinetics and gas phase reactions, utilizing ultraviolet absorption spectroscopy (UVAS). The growth surface conditions are monitored through the back side of the sapphire substrate, utilizing principal angle reflectance spectroscopy (PARS) and laser light scattering (LLS).[16,20,26] For the growth results presented here, the reactor pressures were kept constant at 10 bar, with the main nitrogen flow rate varying from 2 to 6 slm. The precursor flow was evaluated for molar ratio ammonia to TMI, $R_{NH_3:TMI}$, from 500 to 5000. The precursor decomposition kinetics under these growth conditions have been reported previously.[20,21]

III. REAL-TIME OPTICAL CHARACTERIZATION OF INN GROWTH

The decomposition studies for ammonia[20,21] suggest temperatures well above 900 K for sufficient cracking of the ammonia precursor for the growth of InN. It also showed that the observed onset of ammonia decomposition temperature decreases with increasing reactor pressure. Figure 2 shows the PAR and LLS traces recorded for the wavelength $\lambda = 6328$ Å, during InN growth under HCVD conditions. The reactor pressure was maintained at 10 bar, the nitrogen main flow at 6 slm, and the molar ratio ammonia to TMI was 2000. The growth run depicted in Fig. 2 shows a low and even declining LLS signal, while the interference oscillations in the PAR signal show the overall layer growth. Superimposed on the PAR interference oscillations is a fine structure (not resolved) that is strongly correlated to the time sequence of the supply of precursors employed and provide information of the growth surface chemistry and kinetics. Each peak in the fine structure corresponds to a complete precursor cycle sequence. The LLS trace indicates that the surface roughness during growth remains low and even slightly decreases. Based on the analysis of the PAR signal, the average growth rate and the difference between the dielectric functions of film and substrate can be analyzed. The growth rate is estimated to 1.346 Å per cycle sequence. An *ex situ* analysis of the optical properties is given further later.

In Fig. 3 the observed PAR and ultraviolet (UV) transmission traces are shown during the nucleation phase and the steady-state growth of InN. The lower half shows the UV transmission trace recorded for the wavelength $\lambda = 210.8$ nm, monitoring the undecomposed ammonia and TMI species above the growth surface. The PAR trace in the upper half the of the figure is recorded for the wavelength

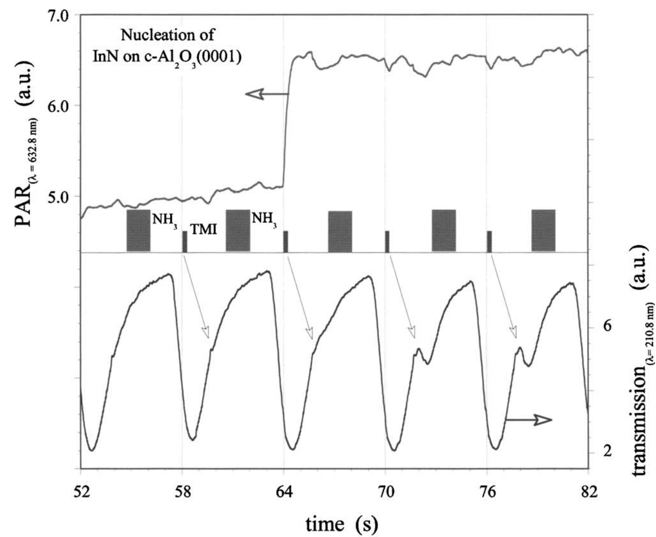

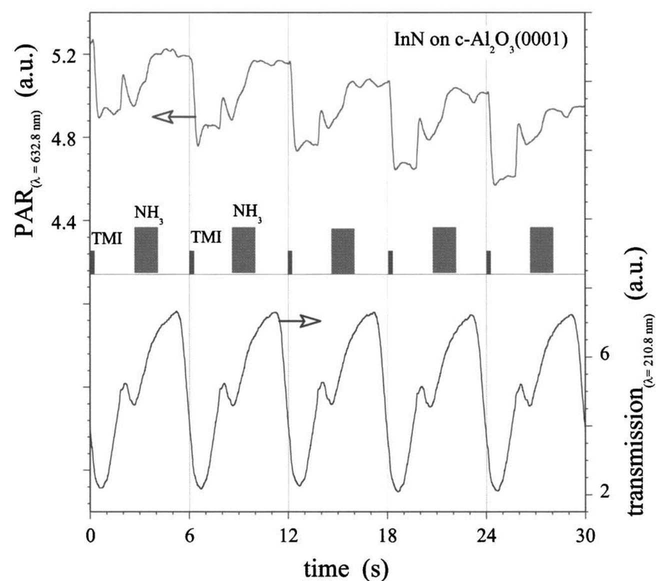

FIG. 3. (a) Monitoring of InN nucleation by PAR and UV transmission traces. A precursor cycle sequence of 6 s with 0.4 s TMI and 1.4 s ammonia pulses, separated by 1.4 s were used. (b) PAR and UV transmission traces during steady-state InN growth at 990 K. The rector pressure was 10 bar with a total flow of 5 slm. The overall decrease in the PAR signal correspond to InN growth.

$\lambda = 6328$ Å, monitoring highly sensitive changes in the dielectric function at the substrate-ambient interface. Also indicated in the figure are the positions of the precursor pulse injections with a total cycle sequence repetition time of 6 s. Note that the precursor injection time and the response seen in UVAS and PAR are temporally shifted according to the average gas velocity in the reactor as mentioned above. As depicted in Fig. 3(a), it takes about one to two cycle sequences before the UV absorption feature for TMI clearly can be observed (see arrows). The PAR signal shows a large increase after the ammonia pulse reaches the substrate, indicating the start of nucleation on InN and the presence of TMI fragments in the surface vicinity. A steady state surface chemistry is typically reached after 5–20 cyclic precursor exposures, depending on substrate temperature, precursor flow ratio, gas phase velocity, and reactor pressure. Figure 3(b) shows the PAR and UVAS responses during steady-state growth conditions. The periodic modulation of the PAR response can be directly correlated to the presence of ammonia and TMI fragments in a surface reaction layer and at the growth surface. The overall decrease in the PAR signal is correlated to the InN growth per cycle sequence as discussed in detail for *p*-polarized reflectance.[26,27]

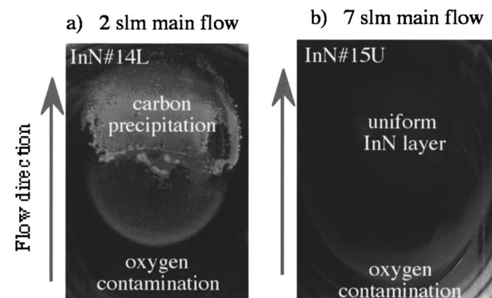

FIG. 4. Influence of gas flow velocity on carbon precipitation/contamination.

Monitoring the PAR response for various growth conditions provides the base for an accurate mapping of the growth parameter space. The results of the decomposition dynamics provide the initial basis for a more detailed understanding of the dissociation of the precursors ammonia and TMI and of the reaction rate constants for growth of InN as theoretical predicted by Cardelino *et al.*[24]

IV. *EX SITU* INN LAYER CHARACTERIZATION

The structural properties of epitaxially grown InN films have been investigated using x-ray diffraction, Auger electron spectroscopy (AES), and Raman spectroscopy. The compositional analysis by AES (including depth profile analysis) shows indium and nitrogen as the main constituents with negligible oxygen concentrations. This was expected, since a reactor overpressure of at least 10 bar and ultrapure gases were used for the InN growth. No correlation with the oxygen content (via AES) with the absorption edge shift was found, confirming studies by Butcher *et al.*,[11] that the incorporation of oxygen does not correlate to changes in the lattice constant.

Spectroscopic techniques such as absorption, reflectance, and spectroscopic ellipsometry, were applied to analyze the optical properties of the InN layers. The absorption spectra observed for a set of growth temperatures and flow velocities are summarized in Fig. 5. For growth temperatures from 900 to 1130 K (sample Nos. 10L, 10u, and 07L) the absorption edge is approximate at 1.85 eV. As the growth temperature is increased an absorption structure around 1.6 develops (see sample Nos. 07L and 12L) and becomes dominant. A further increase leads to a new absorption edge of approximate 0.7 eV (No. 12u).

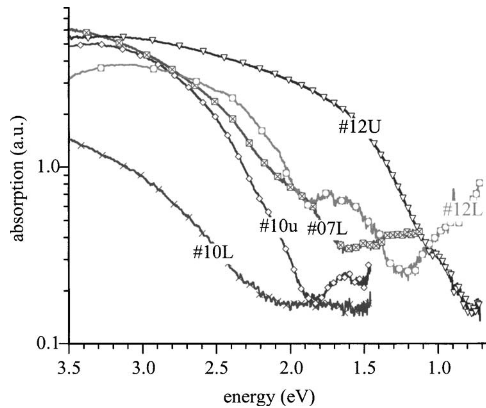

FIG. 5. Absorption spectra for various InN layers grown for various substrate temperatures and flow velocity over the growth substrates. The growth temperature was varied from 1050 up to 1150 K.

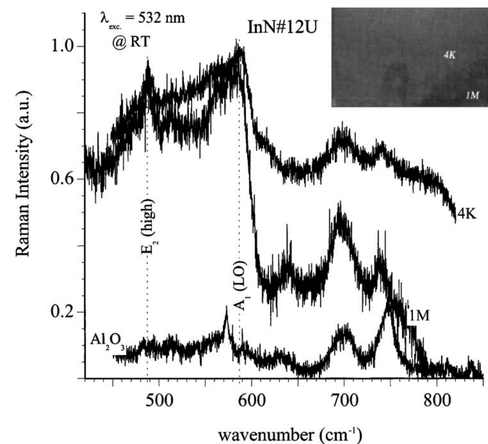

FIG. 6. Raman spectra for the InN layer (InN No. 12U) deposited at 1150 K. The layer has been analyzed at different substrate regions, as indicated in the inset, showing a portion of the InN layer investigated. The analyzed area labeled 1*M* is a smooth goldish-brown InN layer approximate 600 nm thick. The analyzed area labeled 4*K* becomes lightly hazy.

Raman spectroscopy has been applied in order to evaluate the crystallinity of the layers. Layers grown at lower temperatures (900–1100 K) show a broad asymmetric band around 570 cm^{-1}, which can be fitted by Lorentz curves located approximately at 580 and 470 cm^{-1}. Considering the Raman lines E_2(high) and A_1(LO) at 488 and 586 cm^{-1}, respectively,[28–30] both line might be buried under the broad asymmetric band at 570 cm^{-1}. This assumption is supported by Raman spectra obtained for InN layers grown at higher growth temperatures. Figure 6 shows the Raman spectra for an InN layer grown at approximately 1150 K. This layer shows a gradually roughening towards the center of the substrate, which is assumed to be correlated to either an onset of InN etching or an increasingly ammonia depletion. These effects are illustrated by photographs of InN films grown using HPCVD in Fig. 4.

The spectrum labeled "1*M*" was taken at the smooth surface area, while the spectrum labeled "4*K*" was taken at an area with significant surface roughness. From the spectrum 1*M*, we estimate the Raman lines E_2(high) and A_1(LO) at 490 and at 590 cm^{-1}, respectively. The absorption spectrum for this position is shown in Fig. 5 (No. 12U), indicating an absorption edge of approximately 0.7 eV.

V. CONCLUSION

The growth of InN under HPCVD has been introduced. The employed real-time optical growth characterization by UVAS, PAR, and LLS provided crucial insights in the gas phase decomposition kinetics, surface chemistry processes, and the film growth process. We demonstrated that PAR and LLS can follow the film nucleation and growth process the submonolayer resolution, which will be an important tool for engineered nanoscale device structures.

InN layers grown at a reactor pressure of 10 bar for various flow rates and growth temperatures show that crystallinity of the InN layers improves with increasing temperatures. At the same time, an increased growth temperature causes the appearance of an absorption below 1.8 eV and a shifted absorption edge down to 0.7 eV for growth temperatures around 1150 K. The shift in the absorption edge occurs in a very narrow growth temperature region and seems to develop from defect like absorption features centered around 1.6 eV. At present, it is not clear whether the shift in the absorption edge is related to a phase transformation or a significant altered point defect chemistry at higher temperatures. Further studies varying the ammonia to TMI flow ratio, the center flow velocity and the growth temperatures will be needed to understand this periphery-like behavior. An increase in the reactor pressure will allow to push the growth temperature further up, bringing it closer the optimum growth temperature of GaN. This will allow the exploration of indium rich $In_{1-x}Ga_xN$ alloys, presently not possible by MBE or low-pressure OMCVD.

ACKNOWLEDGMENT

The authors would like to acknowledge the support of this work by NASA Grant No. NAG8-1686.

[1]T. Inushima, V. V. Mamutin, V. A. Vekshin, S. V. Ivanov, T. Sakon, M. Motokawa, and S. Ohoya, J. Cryst. Growth **227–228**, 481 (2001).
[2]J. Wu, W. Walukiewicz, W. Shan, K. M. Yu, J. W. Ager III, E. E. Haller, Hai Lu, and William J. Schaff, Phys. Rev. B **66**, 201403 (2002).
[3]R. A. Oliver, C. Nörenberg, M. G. Martin, M. R. Castell, L. Allers, and G. A. D. Briggs, Surf. Sci. **532–535**, 806 (2003).
[4]J. Aderhold *et al.*, J. Cryst. Growth **222**, 701 (2001).
[5]Z. X. Bi *et al.*, Mater. Lett. **58**, 3641 (2004).
[6]J. Wu *et al.*, Appl. Phys. Lett. **80**, 3967 (2002).
[7]I. Vurgaftman and J. R. Meyer, J. Appl. Phys. **94**, 3675 (2003).
[8]V. Yu. Davydov and A. A. Klochikhin, Semiconductors **38**, 861 (2004).
[9]A. G. Bhuiyan, A. Hashimoto, and A. Yamamoto, J. Appl. Phys. **94**, 2779 (2003).
[10]E. Kurimoto, M. Hangyo, H. Harima, M. Yoshimoto, T. Yamaguchi, T. Araki, Y. Nanishi, and K. Kisoda, Appl. Phys. Lett. **84**, 212 (2004).
[11]K. S. A. Butcher *et al.*, J. Appl. Phys. **95**, 6124 (2004).
[12]A. Kasic, E. Valcheva, B. Monemar, H. Lu, and W. J. Schaff, Phys. Rev. B **70**, 115217 (2004).
[13]J. S. Thakur, D. Haddad, V. M. Naik, R. Naik, G. W. Auner, H. Lu, and W. J. Schaff, Phys. Rev. B **71**, 115203 (2005).
[14]V. Yu. Davydov *et al.*, Proc. SPIE **5023**, 68 (2003).

[15]B. Onderka, J. Unland, and R. Schmid-Fetzer, J. Mater. Res. **17**, 3065 (2002).
[16]J. MacChesney, P. M. Bridenbaugh, and P. B. O'Connor, Mater. Res. Bull. **5**, 783 (1970).
[17]O. Ambacher *et al.*, J. Vac. Sci. Technol. B **14**, 3532 (1996).
[18]N. Dietz, S. McCall, and K. J. Bachmann, Proceedings of the Microgravity Conference 2000, NASA/CP-2001-210827, 2001, pp. 176–181.
[19]N. Dietz, V. Woods, S. McCall, and K. J. Bachmann, Proceedings of the Microgravity Conference 2002, NASA/CP-2003-212339, 2003, pp. 169–181.
[20]N. Dietz, H. Born, M. Strassburg, and V. Woods, Mater. Res. Soc. Symp. Proc. **798**, Y10.45.1 (2004).
[21]V. Woods, H. Born, M. Strassburg, and N. Dietz, J. Vac. Sci. Technol. A **22**, 1596 (2004).
[22]V. Woods and N. Dietz, Mater. Sci. Eng., B (submitted).
[23]N. Dietz, M. Strassburg, and V. Woods, J. Vac. Sci. Technol. A (in press).
[24]K. J. Bachmann, S. McCall, S. LeSure, N. Sukidi, and F. Wang, J. Jpn. Soc. Microgravity Appl. **15**, 436 (1998).
[25]S. D. McCall and K. J. Bachmann, Mater. Res. Soc. Symp. Proc. **693**, 13.13.1 (2002).
[26]B. H. Cardelino, C. E. Moore, C. A. Cardelino, S. D. McCall, D. O. Frazier, and K. J. Bachmann, J. Phys. Chem. A **107**, 3708 (2003).
[27]B. H. Cardelino, C. E. Moore, S. D. McCall, C. A. Cardelino, N. Dietz, and K. J. Bachmann, CAITA-2004, Purdue University, June 2004, ISBN 86-7466-117-3, 2004.
[28]N. Dietz, Mater. Sci. Eng., B **87**, 1 (2001).
[29]N. Dietz and K. J. Bachmann, Vacuum **47**, 133 (1996).
[30]V. Y. Davydov *et al.*, Appl. Phys. Lett. **75**, 3297 (1999).